

# Discovery of Spectral Variability of Markarian 421 at TeV Energies

F. Krennrich<sup>1</sup>, I.H. Bond<sup>2</sup>, S.M. Bradbury<sup>2</sup>, J.H. Buckley<sup>3</sup>, D.A. Carter-Lewis<sup>1</sup>, W. Cui<sup>4</sup>,  
I. de la Calle Perez<sup>2</sup>, D.J. Fegan<sup>5</sup>, S.J. Fegan<sup>6,15</sup>, J.P. Finley<sup>4</sup>, J.A. Gaidos<sup>4</sup>, K. Gibbs<sup>6</sup>,  
G.H. Gillanders<sup>7</sup>, T.A. Hall<sup>1,16</sup>, A.M. Hillas<sup>2</sup>, J. Holder<sup>2</sup>, D. Horan<sup>6</sup>, M. Jordan<sup>3</sup>,  
M. Kertzman<sup>8</sup>, D. Kieda<sup>9</sup>, J. Kildea<sup>5</sup>, J. Knapp<sup>2</sup>, K. Kosack<sup>3</sup>, M.J. Lang<sup>7</sup>, S. LeBohec<sup>1</sup>,  
P. Moriarty<sup>10</sup>, D. Müller<sup>11</sup>, R.A. Ong<sup>12</sup>, R. Pallassini<sup>2</sup>, D. Petry<sup>1</sup>, J. Quinn<sup>5</sup>, N.W. Reay<sup>13</sup>,  
P.T. Reynolds<sup>14</sup>, H.J. Rose<sup>2</sup>, G.H. Sembroski<sup>4</sup>, R. Sidwell<sup>13</sup>, N. Stanton<sup>13</sup>, S.P. Swordy<sup>11</sup>,  
V.V. Vassiliev<sup>9</sup>, S.P. Wakely<sup>11</sup>, T.C. Weekes<sup>6</sup>

---

<sup>1</sup>Department of Physics and Astronomy, Iowa State University, Ames, IA 50011

<sup>2</sup>Department of Physics, University of Leeds, Leeds, LS2 9JT, Yorkshire, England, UK

<sup>3</sup>Department of Physics, Washington University, St. Louis, MO 63130

<sup>4</sup>Department of Physics, Purdue University, West Lafayette, IN 47907

<sup>5</sup>Physics Department, National University of Ireland, Belfield, Dublin 4, Ireland

<sup>6</sup> Fred Lawrence Whipple Observatory, Harvard-Smithsonian CfA, Amado, AZ 85645

<sup>7</sup>Physics Department, National University of Ireland, Galway, Ireland

<sup>8</sup>Physics Department, De Pauw University, Greencastle, IN, 46135

<sup>9</sup>High Energy Astrophysics Institute, University of Utah, Salt Lake City, UT 84112

<sup>10</sup>School of Science, Galway-Mayo Institute of Technology, Galway, Ireland

<sup>11</sup>Enrico Fermi Institute, University of Chicago, Chicago, IL 60637

<sup>12</sup>Department of Physics, University of California, Los Angeles, CA 90095

<sup>13</sup>Department of Physics, Kansas State University, Manhattan, KS 66506

<sup>14</sup>Department of Physics, Cork Institute of Technology, Cork, Ireland

<sup>15</sup>Department of Physics, University of Arizona, Tucson, AZ 85721

<sup>16</sup>Department of Physics & Astronomy, University of Arkansas at Little Rock, AR 72204

Received \_\_\_\_\_; accepted \_\_\_\_\_

to appear in the *Astrophysical Journal*

## ABSTRACT

The detection of spectral variability of the  $\gamma$ -ray blazar Mrk 421 at TeV energies is reported. Observations with the Whipple Observatory 10 m  $\gamma$ -ray telescope taken in 2000/2001 revealed exceptionally strong and long-lasting flaring activity. Flaring levels of 0.4 to 13 times that of the Crab Nebula flux provided sufficient statistics for a detailed study of the energy spectrum between 380 GeV and 8.2 TeV as a function of flux level. These spectra are well described by a power law with an exponential cutoff:  $\frac{dN}{dE} \propto E^{-\alpha} \times e^{-E/E_0} \text{ m}^{-2} \text{ s}^{-1} \text{ TeV}^{-1}$ .

There is no evidence for variation in the cutoff energy with flux, and all spectra are consistent with an average value for the cutoff energy of 4.3 TeV. The spectral index varies between  $1.89 \pm 0.04_{\text{stat}} \pm 0.05_{\text{syst}}$  in a high flux state and  $2.72 \pm 0.11_{\text{stat}} \pm 0.05_{\text{syst}}$  in a low state.

The correlation between spectral index and flux is tight when averaging over the total 2000/2001 data set. Spectral measurements of Mrk 421 from previous years (1995/96 and 1999) by the Whipple collaboration are consistent with this flux-spectral index correlation, which suggest that this may be a constant or a long-term property of the source. If a similar flux-spectral index correlation were found for other  $\gamma$ -ray blazars, this universal property could help disentangle the intrinsic emission mechanism from external absorption effects.

*Subject headings:* BL Lacertae objects: individual (Markarian 421) — gamma rays: observations

## 1. INTRODUCTION

The discovery of more than 70 active galactic nuclei (AGNs) by the EGRET  $\gamma$ -ray detector (Hartman et al. 1999) operating at  $E > 30$  MeV gave a fresh perspective on the AGN phenomenon, particularly relevant to understanding the intrinsic properties of their jets. EGRET-detected AGNs are typically radio-loud and show a second peak in their  $\nu F_\nu$  distribution at GeV energies. Blazars detected at TeV energies have a primary peak at X-ray energies and a second component at TeV energies. Both types are  $\gamma$ -ray blazars and the commonly-accepted model is that they have their jet oriented towards the observer revealing emission regions that are strongly Doppler-boosted. Relativistic boosting gives rise to large flux variations (Catanese et al. 1997) and short time scale phenomena (Gaidos et al. 1996). Two AGNs (Mrk 421 and Mrk 501) show emission extending to energies greater than 10 TeV (Aharonian et al. 1999; Krennrich et al. 2001).

Since the discovery of TeV  $\gamma$ -rays from the blazars Mrk 421 (Punch et al. 1992) and Mrk 501 (Quinn et al. 1996), these objects played a significant role in discussions involving the emission processes in AGN jets and attenuation effects of TeV  $\gamma$ -rays propagating over extragalactic distances. Both blazars exhibit episodes of strong flaring activity, providing good statistics for detailed measurements of their average energy spectra from 260 GeV up 17 TeV using ground-based  $\gamma$ -ray telescopes. Mrk 421 and Mrk 501 are at approximately the same distance ( $z=0.031$  and  $z=0.034$ , respectively). Since the level of attenuation of  $\gamma$ -rays by the diffuse extragalactic background light (EBL) via pair creation (Nikishov 1962; Gould & Schröder 1967; Stecker, De Jager & Salamon 1992) depends on the distance of the source to the observer, it could cause a common spectral feature in the energy spectra of Mrk 421 and Mrk 501.

Measurements by the Whipple collaboration (Samuelson et al. 1998; Krennrich et al. 2001) imply that the energy spectra of both Mrk 501 and Mrk 421 require a curved

fit parametrization, e.g., a power law with an exponential cutoff with cutoff energies of  $4.6 \pm 0.8_{\text{stat}}$  TeV and  $4.3 \pm 0.3_{\text{stat}}(-1.4 + 1.7)_{\text{syst}}$  TeV (“stat” means statistical error, “syst” means systematic error), respectively. Data from the HEGRA collaboration suggest that the cutoff energy of Mrk 501 is  $6.2 \pm 0.4_{\text{stat}}(-1.5 + 2.9)_{\text{syst}}$  TeV (Aharonian et al. 1999; Aharonian et al. 2001) and that Mrk 421 has a cutoff energy of  $4.2 (+0.6 - 0.4)_{\text{stat}}$  TeV (Kohnle et al. 2001). The results from the two groups may be consistent given systematic uncertainties. The interpretation of the origin of the cutoff requires a better understanding of the emission process in  $\gamma$ -ray blazars as a class of objects. Making progress in unraveling the emission process in blazars from external attenuation effects requires two types of key observations.

The first is contemporaneous multiwavelength observations at X-ray and TeV energies (see Buckley et al. 1996; Krawczynski et al. 2002). These constrain the emission process by simultaneously probing the synchrotron emission and the mechanism responsible for the  $\gamma$ -ray component, e.g., the inverse Compton scattering process (Maraschi, Ghisellini & Celotti 1992; Marscher & Travis 1996). There are also competing models that assume that the high energy emission arises from protons (Mannheim 1998; Mücke & Protheroe 2001; Aharonian 2000).

The second is the study of  $\gamma$ -ray spectral variability as a function of flux and time. Spectral variability is directly tied to the emission process at the source, whereas external absorption by the EBL is a universal feature that is independent of flux level. Thus, by studying the spectral variability, we are able to disentangle these two effects. In synchrotron-Compton models, spectral variability could be explained by cooling of electrons in the jet causing a shift of the break in the electron spectrum, or by variations of the maximum energy of accelerated electrons. Spectral variability may also be a key to the understanding of the energy dissipation processes in the vicinity of a supermassive black

hole powering the jet.

Some evidence for spectral variability has been reported by Djannati-Ataï et al. (1999) and Krawczynski et al. (2001) for Mrk 501; however, the effect was not highly statistically significant ( $\approx 4$  standard deviations) and precluded detailed studies. In fact, the spectral index of Mrk 501 turned out to be surprisingly stable during observations of a strong outburst in 1997 (Aharonian et al. 1999) though the flux varied by a factor of 30.

In this paper we present the discovery of spectral variability of Mrk 421 at TeV energies based on data taken with the Whipple Observatory 10 m  $\gamma$ -ray telescope. We show that Mrk 421 exhibits a remarkable flux-spectral index correlation that appears to be stable averaged over time-scales of months to several years.

## 2. OBSERVATIONS & DATA ANALYSIS

The observations were made with the Whipple Observatory 10 m  $\gamma$ -ray telescope using the GRANITE-III high-resolution camera (Finley et al. 2001). The high sensitivity of the telescope for point sources in the energy range from  $\approx 200$  GeV to greater than 20 TeV permits the measurement of energy spectra of  $\gamma$ -ray sources with fluxes above 1 Crab on time-scales as short as 30 minutes (1 Crab is defined as the differential flux of the Crab Nebula at 1 TeV in photons  $\text{m}^{-2} \text{s}^{-1} \text{TeV}^{-1}$ ).

Mrk 421 was more active in the 2000/2001 observing season than in previous years. Unusually high flaring states ranging from 0.4 Crab to 13 Crab, lasting for a period of approximately five months, provided a wealth of statistics for studies of spectral variability. The data used for the analysis in this paper were collected on 2000 November 28, December 4-6, 22, 27, 28-29 and 2001 January 20-21, 24-25, 30-31, February 1-3, 19, 27-29, March 19, 22-23, 26-27, 30 and April 13. These data are an extension to the data set published in

Krennrich et al. (2001), and include observations of the source in a lower flux state. A total of 49.93 hours of on-source observation time with zenith angles less than  $\approx 35^\circ$  has been used in this study.

The  $\gamma$ -ray rate of the 107 individual on-source runs varies from 0.4 to 18.0  $\gamma$  minute<sup>-1</sup>. The background from cosmic-ray induced showers has been estimated for each on-source run individually by using a matching off-source run also taken during the 2000/2001 season. A good match requires that both runs cover a similar zenith angle range, and that the on-source and off-source runs show good agreement in the distribution of the parameter associated with the alignment of the image in the focal plane, for values of the parameter outside the  $\gamma$ -ray fiducial region. In some runs, a normalization factor between the on and off samples was applied to ensure that the off-samples accurately represented the background in the on-region. This procedure has been tested as a function of the total light intensity of the  $\gamma$ -ray image to minimize a possible systematic bias. Uncertainties in the spectral index, alpha, due to the method of background estimation are typically  $\Delta\alpha < 0.1$  in the spectral index for individual runs and  $\Delta\alpha < 0.05$  for sets of 5 or more runs.

In a search for yearly trends in a flux-spectral index correlation we also include previously published data from 1995 and 1996 (Krennrich et al. 1999a). In addition we derive a spectrum for observations taken in May-June 1999 using the GRANITE-III 331-pixel camera (Krennrich et al. 1999b; Le Bohec et al. 2000; Finley et al. 2001). The data consist of 33 on-source and 33 matched off-source runs from 1999 May 6-7, 9-10, 11, 16-18 and 1999 June 5-8.

The analysis methods for the 2000/2001 observations,  $\gamma$ -ray selection and energy estimate are based on the method described in Mohanty et al. (1998) and their application has been described in Krennrich et al. (2001). These  $\gamma$ -ray selection criteria are derived from parameter distributions of simulated  $\gamma$ -ray showers as a function of their total light

intensity in the camera. We set these criteria so that they retain 90% of  $\gamma$ -ray images whose centroid is within  $0.4^\circ - 1.0^\circ$  from the center of the camera. To avoid the difficulties of modeling the trigger electronics we apply an additional cut requiring that a signal of at least 15.1, 13.6, and 12.1 photoelectrons are present in the three highest camera pixels, respectively. In this analysis, we have increased the lowest energy point of our spectral measurements from 260 GeV to 380 GeV, to minimize the systematic uncertainties inherent at low energies.

### 3. RESULTS: SPECTRAL VARIABILITY AS A FUNCTION OF FLUX

The data were divided a priori into eight independent subsets with comparable numbers of excess events and average  $\gamma$ -ray rates ranging from 3.3 to 16.0  $\gamma$  minute<sup>-1</sup>. In Figure 1 we show the corresponding energy spectra. For clarity of presentation we have combined set II and III, and set VI and VII, respectively. Progressive hardening of the spectra is apparent to the eye when comparing the spectra towards increasing flux levels. We have attempted to fit the individual spectra by a simple power law. These fits result in unacceptable goodness of fit ( $\chi^2$ ) values for sets I-IV, hence the power law hypothesis is rejected (also see Table 1).

For comparison with previous papers (Krennrich et al. 1999a; Krennrich et al. 2001) and the results from other groups (Piron et al. 2001; Bazer-Bachi et al. 2001), we also fit the data using a parabolic function:  $\frac{dN}{dE} \propto E^{-\alpha - \beta \log_{10}(E)} \text{ m}^{-2} \text{ s}^{-1} \text{ TeV}^{-1}$ . The results in Table 2 have acceptable goodness of fit ( $\chi^2$ ) values. The spectrum hardens with increasing flux, whereas the curvature term shows no significant dependence on flux. In a previous paper (Krennrich et al. 2001) describing the average energy spectrum of Mrk 421 in a high flaring state in 2001, the best fit to the energy spectrum was achieved by using a power law with an exponential cutoff.



$$(1) \quad \frac{dN}{dE} \propto E^{-\alpha} \times e^{-E/E_0} \text{ m}^{-2} \text{ s}^{-1} \text{ TeV}^{-1}$$

The results for fits of this form are provided in Table 3 and exhibit acceptable goodness of fit values for all spectra. Since the spectral index and cutoff energy  $E_0$  are correlated, we also present the uncertainty of  $E_0$  when accounting for this correlation as shown in parenthesis in Table 3. These uncertainties are the extrema of  $E_0$  of the  $1 \sigma$  error ellipse<sup>1</sup> that result from plotting the minimizing function  $\chi^2$  as a function of spectral index  $\alpha$  versus cutoff energy  $E_0$ .

Figure 2 shows the derived cutoff energies for the individual data sets (I-VIII) at different flux levels in units of Crab. No evidence for variability in the cutoff energy is suggested by the data (probability for the hypothesis of a fixed cutoff energy is  $P = 0.98$ ). It is, however, important to realize that the statistical uncertainties in the cutoff energy are strongly correlated with the spectral index and the error bars on  $E_0$  are typically of magnitude 1-3 TeV. Therefore, we cannot exclude variability in the cutoff energy at the few TeV level. Instruments that extend to significantly lower energies and provide better sensitivity at higher energies are required to reduce the uncertainties in the cutoff energy. In addition, our measurement of the cutoff energy has systematic uncertainties, e.g., the absolute energy scale, which can also be improved with the next generation of  $\gamma$ -ray instruments, the VERITAS project (Weekes et al. 2002).

Hence, for the remainder of this paper we adopt a parametrization (see equation 2) with a fixed cutoff energy of  $E_0 = 4.3$  TeV, the same cutoff energy that was derived for the average spectrum of Mrk 421 in a high flaring state (Krennrich et al. 2001).

$$(2) \quad \frac{dN}{dE} \propto E^{-\alpha} \times e^{-E/E_0} \text{ m}^{-2} \text{ s}^{-1} \text{ TeV}^{-1} \text{ with } E_0 = 4.3 \pm 0.3_{\text{stat}} (-1.4 + 1.7)_{\text{syst}} \text{ TeV}$$

---

<sup>1</sup>as calculated by MINUIT, Version 94.1, Cern Program Library entry D506. We also compared MINUIT with the method given by Avni et al. (1976) giving consistent results.

As can be seen from Table 3, the spectra corresponding to different flux levels are well fit by this parametrization, but show significant variation in the spectral index  $\alpha$ . We find that the energy spectra exhibit spectral variability from  $\alpha = 1.89 \pm 0.04_{\text{stat}} \pm 0.05_{\text{sys}}$  up to  $\alpha = 2.72 \pm 0.11_{\text{stat}} \pm 0.05_{\text{sys}}$ . The systematic uncertainties, which are indicated by the shaded areas in Figure 1, have been derived as in Krennrich et al. (2001) by varying cut efficiencies, the angular resolution cut and the software trigger threshold. In addition, uncertainties due to the method of background matching are included. Other potential sources of systematic uncertainties such as throughput variations (light throughput of the atmosphere, mirror reflectivity and gain variations of the telescope) (see LeBohec & Holder 2002, in preparation), elevation dependence and varying signal-to-background ratio have been studied. No systematic dependence of the spectral index with these variables were found.

Figure 3 shows the spectral index as a function of the absolute  $\gamma$ -ray flux in units of the Crab. Variability of the spectral index is apparent, and therefore the hypothesis that the spectral index is constant can be excluded at the  $P = 9.5 \times 10^{-14}$  level. The correlation between spectral index and flux indicates substantial spectral hardening with increasing flux. If we fit the spectral index as a function of flux  $\Phi$  in units of Crab with a second order polynomial we get

$$\alpha(\Phi) = -2.66 (\pm 0.01) + 0.123 (\pm 0.030) \times [\Phi/\text{Crab}] - 0.0056 (\pm 0.00230) \times [\Phi/\text{Crab}]^2$$

which provides a  $\chi^2 = 13.92$  for 5 degrees of freedom ( $P = 1.61 \times 10^{-2}$ ).

#### 4. DISCUSSION

Strong and extended flaring of Mrk 421 allows us to study the spectral variability of this source as a function of flux. Averaged over the time period 2000 November 28 to

2001 April 13 the data show a clear flux-spectral index correlation, with the spectral index varying between  $1.89 \pm 0.04$  in a high state and  $2.72 \pm 0.11$  in a low state.

Whether or not this correlation is maintained in different epochs outside of the 2000/2001 observing period can be addressed using previously published results and archival data from the Whipple collaboration. Figure 3 also shows results from the average spectrum in 1995/1996 in a high state (Krennrich et al. 1999a) and the average spectrum from 1999 May 6 through June 8. The data points from 1995/1996 and from 1999 fall into place with the flux-spectral index correlation as observed for the 2000/2001 data alone. This indicates that the correlation between spectral index and flux holds true when averaging over time scales of months to five years.

Spectral hardening during flares has also been observed for Mrk 421 in X-rays by Fossati et al. (2000) using BeppoSAX data during X-ray flares in 1997 and 1998. In X-rays, the effect of spectral hardening has been interpreted as a shift of the synchrotron peak towards higher frequencies. The flux-spectral index correlation seen in the TeV spectra could also be interpreted as a shift of the high energy peak towards higher frequencies. The shape of the spectrum I in Figure 1 suggests that the peak in  $\nu F_\nu$  is at a few hundred GeV, significantly above previous levels (Maraschi et al. 1999). The spectral hardening is most evident at energies below 2 TeV; it is not uniform.

Strong spectral hardening at lower energies might be expected in the inverse-Compton (IC) scenario in which the IC peak shifts towards higher energies as the flux increases. Conversely, at the higher energies, spectral softening occurs due to either a terminating particle distribution in energy, the falling cross-section due to the Klein-Nishina effect, or external attenuation effects from the EBL or nearby radiation fields. If the changes are due to a shifting IC peak energy, the flux value would be closely tied to the spectral index, as seen here. Further studies of spectral variability on short time-scales (hours-days) will be

presented in a follow-up paper.

We acknowledge the technical assistance of K. Harris, J. Melnick and E. Roache. This research is supported by grants from the U.S. Department of Energy and by NASA, NSF, and by PPARC in the UK and by Enterprise-Ireland.

## REFERENCES

- Aharonian, F.A., et al. 1999, *A&A*, 349, 11
- Aharonian, F. A. 2000, *New Astronomy*, 5, 377
- Aharonian, F.A., et al. 2001, *A&A*, 366, 62
- Avni, Y. 1976, *ApJ*, 210, 642
- Bazer-Bachi, R., et al. 2001, in *AIP Conf. Proc. 558, High Energy Gamma-Ray Astronomy*, ed. F.A. Aharonian & H.J. Völk (New York:AIP), 643
- Buckley, J.H., et al. 1996, *ApJ*, 472, L9
- Catanese, M.A., et al. 1997, *ApJ*, 487, L143
- Djannati-Ataï, A., et al. 1999, *A&A*, 350, 17
- Finley, J.P., et al. 2001, *Proc. 27th Int. Cosmic-Ray Conf. (Hamburg)*, 2827
- Fossati, G., et al. 2000, *ApJ*, 541, 166
- Gaidos, J. A., et al. 1996, *Nature*, 383, 319
- Gould, R. J., & Schréder, G. 1967, *Phys. Rev.*, 155, 1408
- Hartman, R.C., et al. 1999, *ApJS*, 123, 79
- Kohnle, A., et al. 2001, *Proc. of 27th Int. Cosmic-Ray Conf. (Hamburg)*, 2605
- Krawczynski, H., et al. 2001, *High Energy Gamma-Ray Astronomy, AIP Conf. Proc.*, 558  
eds. F.A. Aharonian & H.J. Völk, 639
- Krawczynski, H., et al. 2002, *M.N.R.A.S.*, in press

- Krennrich, F., et al. 1999a, *ApJ*, 511, 149
- Krennrich, F., et al. 1999b, *Proc. of 26th Int. Cosmic-Ray Conf. (Salt Lake City)*, 3, 301
- Krennrich, F., et al. 2001, *ApJ*, 560, L45
- LeBohec, S., et al. 2000, *ApJ*, 539, 209
- Mannheim, K. 1998, *Science*, 279, 684
- Maraschi, L., Ghisellini, G., & Celotti, A. 1992, *ApJ*, 397, L5
- Maraschi, L., et al. 1999, *ApJ*, 526, L81
- Marscher, A.P., & Travis, J.P. 1996, *A&AS*, 120, 537
- Mohanty, G., et al. 1998, *Astropart. Phys.*, 9, 15
- Mücke, A., & Protheroe, R.J. 2000, *Astropart. Phys.*, 15, 121
- Nikishov, A.I. 1962, *Soviet Phys.—JETP Lett.*, 14, 393
- Piron, F., et al. 2001, *A&A*, 374, 895
- Punch, M., et al. 1992, *Nature*, 358, 477
- Quinn, J., et al. 1996, *ApJ*, 456, L83
- Samuelson, F. W., et al. 1998, *ApJ*, 501, L17
- Stecker, F. W., De Jager, O. C., & Salamon, M. H. 1992, *ApJ*, 390, L49
- Weekes, T.C., et al. 2002, *Astropart.Phys.*, 17, 221

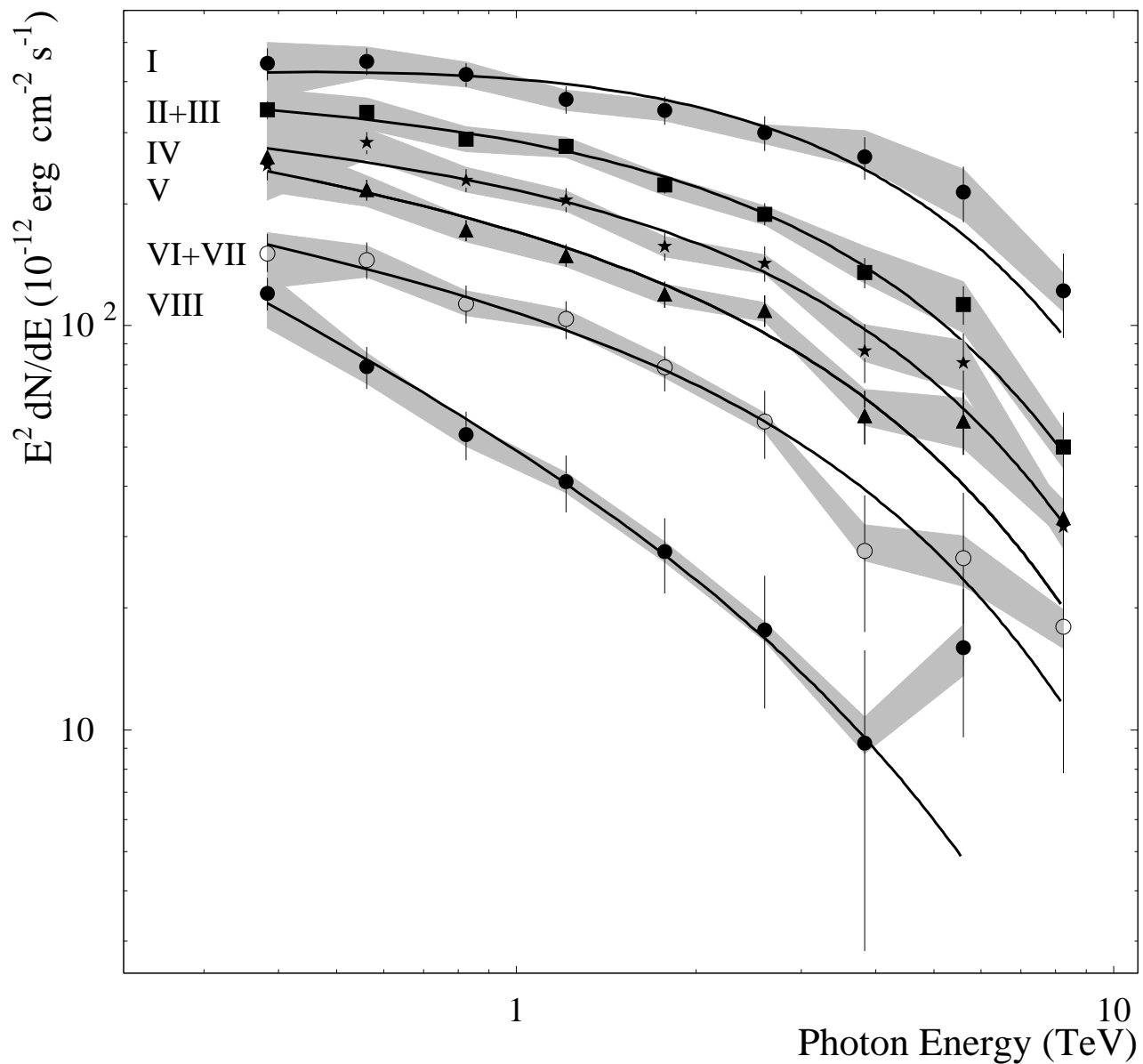


Fig. 1.— Mrk 421 spectra at different flux levels averaged for data over the 2000/2001 season. The spectra have been fit by a power law with a fixed exponential cutoff at 4.3 TeV (Krennrich et al. 2001). The fits produce acceptable goodness of fit ( $\chi^2$ ) values. The shaded areas indicate the systematic errors on the flux measurements.

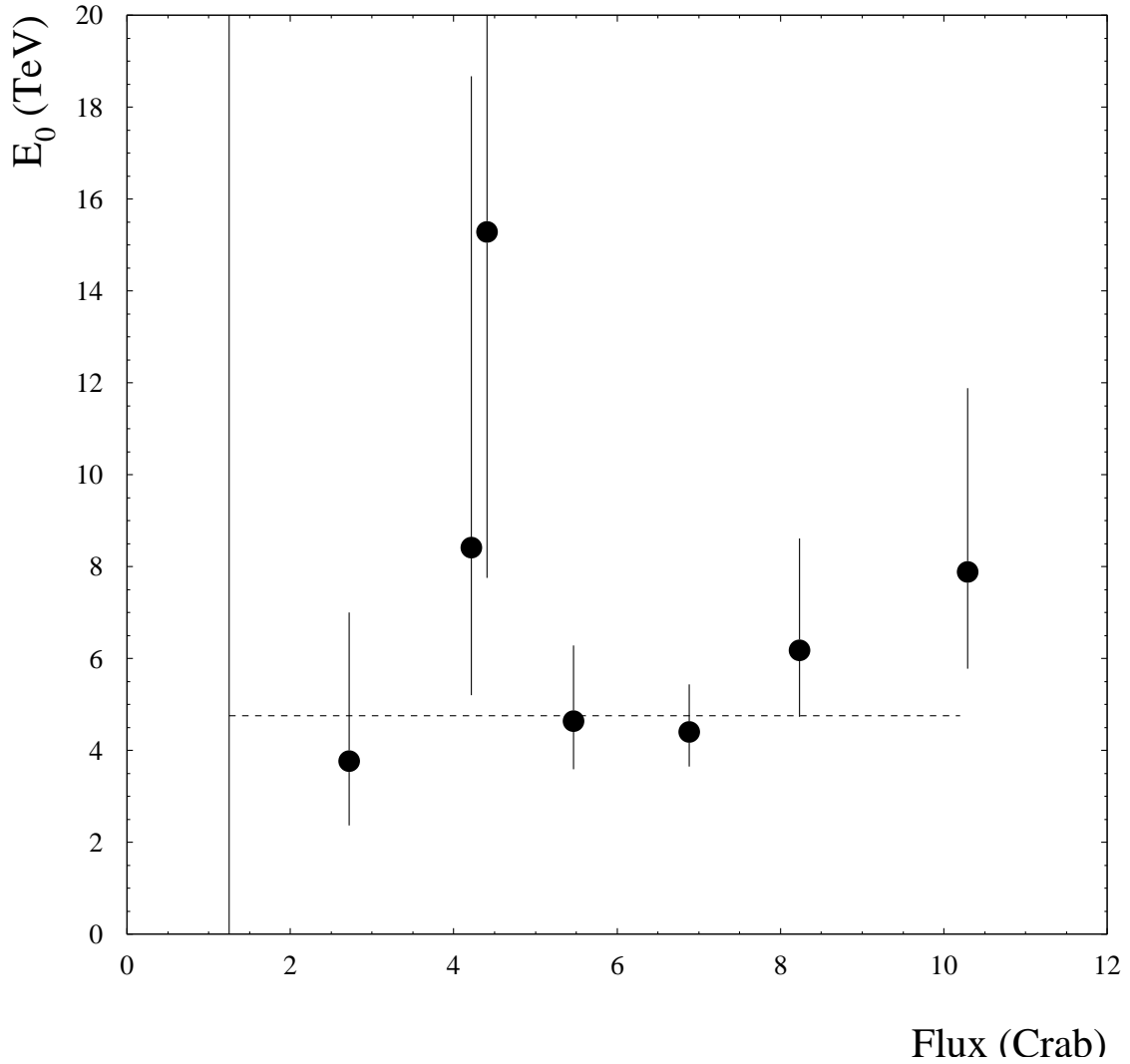


Fig. 2.— The cutoff energy  $E_0$  is plotted as a function of flux in units of Crab (defined in text) for various flaring states (data sets I-VIII) of the 2000/2001 season. No significant variability of the cutoff energy is seen in the data. Note that the point at the lowest flux level has a large statistical uncertainty so that it is off the plot, only showing its error bar.



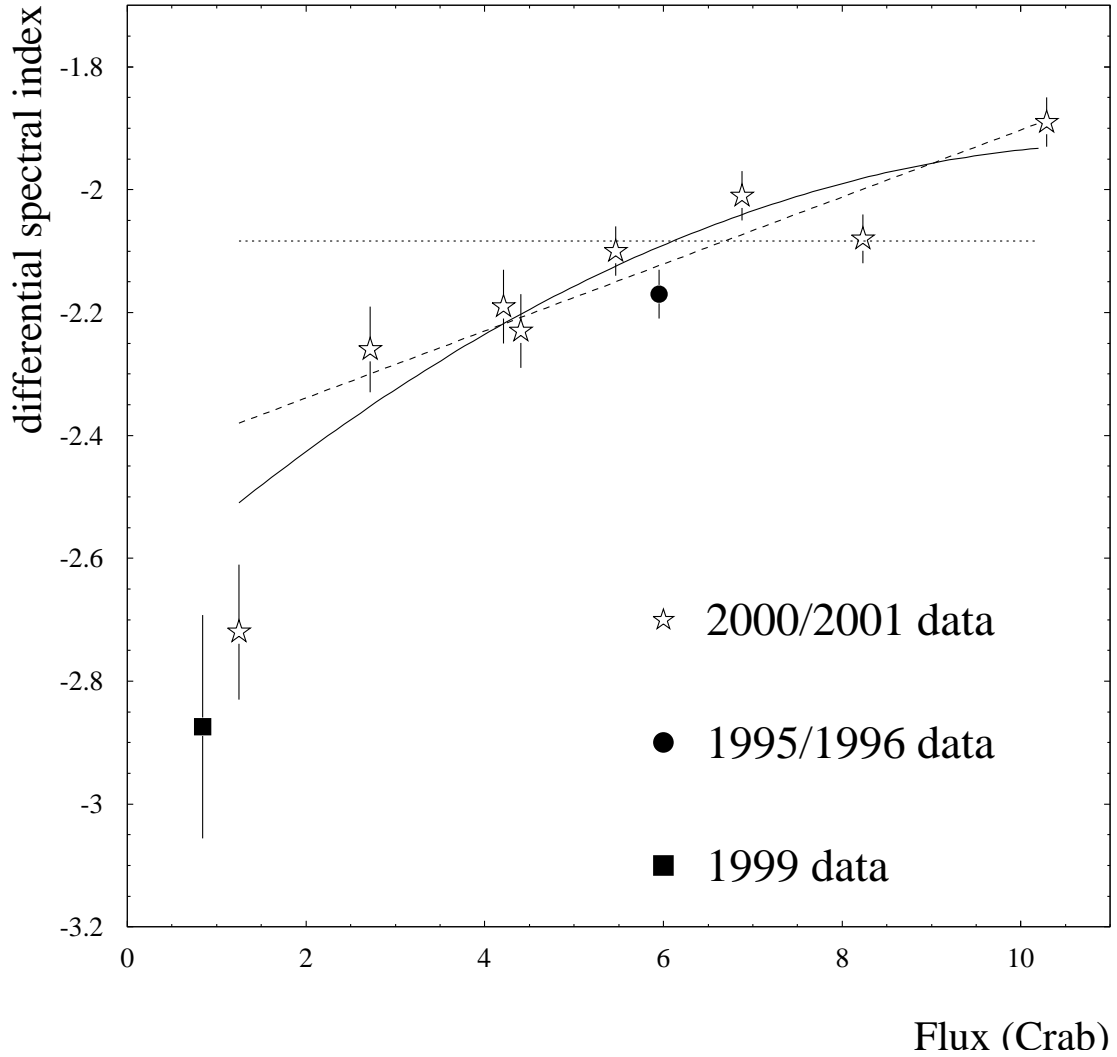


Fig. 3.— The stars show the spectral index of Mrk 421 as function of flux (in Crab units) for the 2000-2001 data set. The hypothesis of a constant spectral index (dotted line) is rejected, whereas the data are better fit by a linear relation ( $P = 5 \times 10^{-3}$ ). A second order polynomial (solid line) gives a better but still marginal fit ( $P = 1.6 \times 10^{-2}$ ). In addition,

we show results for Whipple 1995/96 data (solid circle) from Krennrich et al. (1999a) and data taken during 1999 May-June (solid rectangle).

Table 1. Fits to the spectra of Mrk 421: power law<sup>a</sup>

set	$\alpha$	$\chi^2/\text{dof}^b$
I	$2.31 \pm 0.04$	1.57
II	$2.47 \pm 0.03$	3.70
III	$2.43 \pm 0.03$	5.47
IV	$2.48 \pm 0.06$	3.86
V	$2.56 \pm 0.05$	0.91
VI	$2.57 \pm 0.04$	0.82
VII	$2.60 \pm 0.06$	1.28
VIII	$2.95 \pm 0.10$	0.32

<sup>a</sup>  $dN/dE \propto E^{-\alpha}$  ( $\text{m}^{-2} \text{s}^{-1} \text{TeV}^{-1}$ )

<sup>b</sup> Results from the fits for the energy spectra of Mrk 421, using a power law.

Table 2. Fits to the spectra of Mrk 421: power law with curvature.

set	parabolic <sup>a</sup>		
	$\alpha$	$\beta$	$\chi^2/\text{dof}^b$
I	$2.22 \pm 0.05$	$0.27 \pm 0.10$	0.40
II	$2.39 \pm 0.04$	$0.34 \pm 0.09$	1.53
III	$2.29 \pm 0.04$	$0.45 \pm 0.09$	0.91
IV	$2.38 \pm 0.05$	$0.45 \pm 0.11$	1.08
V	$2.51 \pm 0.06$	$0.20 \pm 0.13$	0.63
VI	$2.55 \pm 0.05$	$0.13 \pm 0.12$	0.75
VII	$2.53 \pm 0.08$	$0.49 \pm 0.21$	0.32
VIII	$2.95 \pm 0.09$	$-0.16 \pm 0.29$	0.32

<sup>a</sup>  $dN/dE \propto E^{-\alpha-\beta \log_{10} E}$  ( $\text{m}^{-2} \text{s}^{-1} \text{TeV}^{-1}$ )

<sup>b</sup> Results from the fits using a power law fit including curvature.

Table 3. Fits to energy spectra of Mrk 421 at various flux levels in 2001: power law including exponential cutoff.

set	power law exp. cutoff <sup>a</sup>			exp. cutoff (4.3 TeV) <sup>b</sup>	
	$\alpha$	$E_0^c$	$\chi^2/\text{dof}^d$	$\alpha$	$\chi^2/\text{dof}^e$
I	$2.07 \pm 0.09$	$7.89 \pm 2.65 \left( \begin{smallmatrix} +4.1 \\ -2.1 \end{smallmatrix} \right)$	0.23	$1.89 \pm 0.04$	1.04
II	$2.20 \pm 0.08$	$6.18 \pm 1.76 \left( \begin{smallmatrix} +2.4 \\ -1.5 \end{smallmatrix} \right)$	1.75	$2.08 \pm 0.04$	2.13
III	$2.02 \pm 0.08$	$4.40 \pm 0.86 \left( \begin{smallmatrix} +1.0 \\ -0.8 \end{smallmatrix} \right)$	0.30	$2.01 \pm 0.04$	0.34
IV	$2.12 \pm 0.09$	$4.64 \pm 1.27 \left( \begin{smallmatrix} +1.7 \\ -1.1 \end{smallmatrix} \right)$	1.28	$2.10 \pm 0.04$	1.30
V	$2.36 \pm 0.11$	$8.41 \pm 4.61 \left( \begin{smallmatrix} +10.3 \\ -3.2 \end{smallmatrix} \right)$	0.46	$2.19 \pm 0.06$	0.83
VI	$2.46 \pm 0.09$	$15.29 \pm 12.26 \left( \begin{smallmatrix} +100.4 \\ -7.5 \end{smallmatrix} \right)$	0.71	$2.23 \pm 0.06$	1.69
VII	$2.22 \pm 0.19$	$3.77 \pm 2.02 \left( \begin{smallmatrix} +3.2 \\ -1.4 \end{smallmatrix} \right)$	0.43	$2.26 \pm 0.07$	0.44
VIII	$2.95 \pm 0.10$	$25,977 \pm 84,528 \left( \begin{smallmatrix} +10,712 \\ -50,301 \end{smallmatrix} \right)$	0.38	$2.72 \pm 0.11$	0.81

<sup>a</sup>  $dN/dE \propto E^{-\alpha} e^{-E/E_0}$  ( $\text{m}^{-2} \text{s}^{-1} \text{TeV}^{-1}$ )

<sup>b</sup>  $dN/dE \propto E^{-\alpha} e^{-E/E_0}$  ( $\text{m}^{-2} \text{s}^{-1} \text{TeV}^{-1}$ );  $E_0 = 4.3 \text{ TeV}$  fixed

<sup>c</sup> cutoff energy  $E_0$  (TeV)

<sup>d,e</sup> Results from the fits using a power law fit with an exponential cutoff.